

Supplementary Materials: Computed Tomography Radiomics for Residual Positron Emission Tomography-Computed Tomography Uptake in Lymph Nodes after Treatment

Chu Hyun Kim, Hyunjin Park, Ho Yun Lee, Joong Hyun Ahn, Seung-hak Lee, Insuk Sohn, Joon Young Choi and Hong Kwan Kim

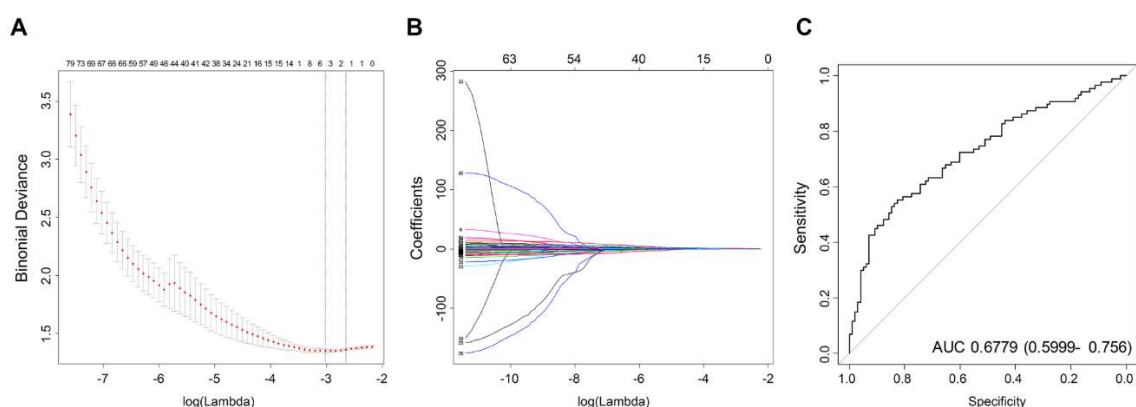


Figure S1. Selection of radiomics features using the least absolute shrinkage and selection operator (LASSO) logistic regression model. (A) LASSO coefficient analysis of 161 radiomics features. (B) Coefficient plotted against the log (λ) sequence. Four nonzero coefficients (indicated by a vertical line in the plot) were selected. (C) Predictive accuracy of the radiomics signature.

Table S1. Radiomics features based on histogram, shape and size, texture, fractal, filters, and sigmoid functions.

| Histogram Features | | Shape and Size Features | Texture Features | | |
|-----------------------|--------------------------|-------------------------|-----------------------|--------------------|----------------|
| Based on Whole Pixels | Based on Positive Pixels | Based on 2D, 3D Images | Based on GLCM | Based on ISZ | Based on NGTDM |
| Maximum* | Mean | Compactness | Auto correlation** | Size zone variance | Busyness |
| Minimum* | Standard variation | Surface area | Cluster tendency** | Intensive variance | Coarseness |
| Median* | Variance | Convexity | Maximum probability** | | Complexity |
| Mean* | Maximum | Sphericity | Contrast** | | Contrast |
| Variance* | Median | Spherical disproportion | Difference entropy** | | Strength |
| Standard variation* | Minimum | Maximum 3D diameter | Dissimilarity** | | |
| Energy | Interquartile range | Surface-to-volume ratio | Energy** | | |
| Skewness* | Range | Volume | Entropy** | | |
| Kurtosis* | Root mean square | Density | Homogeneity** | | |

| Root mean square | Skewness | Mass | Informational measure of correlation** |
|---------------------------------------|---------------------------------|----------------------------|--|
| Inter quartile range | Energy | Roundness factor | Variance** |
| Range | Entropy | Eccentricity | |
| Percentile 2.5%, 25%, 50%, 75%, 97.5% | Kurtosis | Solidity | |
| Entropy* | Uniformity | | |
| Uniformity | | | |
| Mean value of positive pixels | | | |
| Uniformity of positive pixels | | | |
| Fractal Features | | Filtered Features (LoG***) | Sigmoid Function Features |
| Based on the Box-Counting Method | Based on the Blanket Method | $\sigma = 0.5-3.5$ | 3,5,7 mm |
| Dimension | Fractal signature dissimilarity | Mean | Amplitude mean |
| Lacunarity | | Max | Amplitude standard deviation |
| | | Min | Slope mean |
| | | Median | Slope standard deviation |
| | | Standard deviation | Offset mean |
| | | Skewness | Offset standard deviation |
| | | Kurtosis | |
| | | Uniformity | |
| | | Entropy | |

ISZ, intensity variance and size zone variance value; GLCM, gray-level co-occurrence matrix; NGTDM, neighborhood gray tone difference matrix; LoG, Laplacian of Gaussian. *These features were calculated from the whole, inner 2/3, and outer 1/3 of the ROI. Difference (delta) between inner and outer ROIs was computed. **These features were calculated from the setting of * plus sub-sampled ROIs. ***Sigma values for LoG features were computed for $\sigma = 0.5-3.5$ in 0.5 increments.

Table S2. Definitions of extracted radiomics features.

| Category | Parameter | Formula | Description |
|------------------------------|-----------|--|--|
| Histogram-based features [1] | Max, Min | $\text{Max} = \text{Max}(X(i)) \text{ or } \text{Min} = \text{Min}(X(i))$ where X denotes the 3D image matrix with N voxels. | Measures maximum or minimum intensity value of a histogram |
| | Median | $\text{Median} = \frac{X(i)}{2}$ where X denotes the 3D image matrix | Measures median intensity value of a histogram |
| | Mean | $\text{Mean} = \frac{1}{N} \sum_{i=1}^N X(i)$ where X denotes the 3D image matrix with N voxels. | Measures mean intensity value of a histogram |

| | | |
|---|--|---|
| Variance | $\text{Variance} = \frac{1}{N-1} \sum_{i=1}^N (X(i) - \bar{x})^2$ | Measures squared distances of each value of a histogram from the mean |
| Standard deviation | $\text{Std} = \left(\frac{1}{N-1} \sum_{i=1}^N (X(i) - \bar{x})^2 \right)^{1/2}$ <p>where X denotes the 3D image matrix with N voxels.</p> | Measures amount of variation of a histogram. |
| Energy | $\text{Energy} = \sum_i X(i)^2$ <p>where X denotes the 3D image matrix with N voxels.</p> | Measures squared magnitude value of a histogram |
| Skewness | $\text{Skewness} = \frac{E(x - \mu)^3}{\sigma^3}$ <p>where μ is the mean of x, σ is the standard deviation of x, and E is the expectation operator.</p> | Measures asymmetry of a histogram. |
| Kurtosis | $\text{Kurtosis} = \frac{E(x - \mu)^4}{\sigma^4}$ <p>where μ is the mean of x, σ is the standard deviation of x, and E is the expectation operator.</p> | Measures “peakedness” of a histogram (flatness of histogram) |
| Root mean square (RMS) | $\text{RMS} = \sqrt{\frac{1}{N} \sum_{n=1}^N X_n ^2}$ <p>where X denotes the 3D image matrix with N voxels.</p> | Measures the square root of the mean of the squares of the values of the histogram. This feature is another measure of the magnitude of a histogram |
| Interquartile range | $\text{IQR} = Q_3 - Q_1$ <p>where Q_3 denote the 3rd quartile of the histogram, and Q_1 denotes the 1st quartile of the histogram</p> | Measure of variability, based on dividing a histogram into quartiles |
| Range | $\text{Range} = \text{range}(X(i))$ | Measures difference between the highest and lowest voxel values of a histogram |
| Percentile | $\text{Percentile} = \left(\frac{n^{\text{th percentile}}}{100} \right) X(i)$ | Measures intensity value at the 2.5th, 25th, 50th, 75th, and 97.5th percentiles on the histogram |
| Entropy | $\text{Entropy} = - \sum_{i=1}^{N_i} P(i) \log_2 P(i)$ <p>where P denotes the first-order histogram with N_i discrete intensity levels.</p> | Measures irregularity of a histogram. |
| Uniformity | $\text{Uniformity} = \sum_{i=1}^{N_i} P(i)^2$ <p>where P denotes the first-order histogram with N_i discrete intensity levels.</p> | Measures uniformity of a histogram. |
| Mean value of positive pixels (MPP) | $\text{MPP} = \frac{1}{N_+} \sum_i X(i)$ <p>where N_+ denotes the total number of positive gray level pixels in X(i)</p> | Measures average positive histogram value. |
| Uniformity value of positive pixels (UPP) | $\text{UPP} = \sum_{i=1}^{N_i} P(i) ^2$ | Measures uniformity of a positive histogram value. |

| | | | |
|--|-------------------------------|---|--|
| | | where P denotes the first-order histogram with N_l discrete intensity levels. | |
| Shape- and physical-based features [1,2] | Compactness | $\text{Compactness} = \frac{V}{\sqrt{\pi}A^{\frac{2}{3}}}$ <p>where V denotes the volume and A denotes the surface area of the volume of interest (VOI)</p> | Quantifies how close an object is to the smoothest shape, the circle |
| | Surface area | $SA = \sum_{i=1}^N \frac{1}{2} a_i b_i \times a_i c_i $ <p>where N is the total number of triangles (covered surface area), and a, b, c are edge vectors</p> | Surface area of the ROI |
| | Convexity | $\text{Convexity} = \frac{V}{V'}$ <p>where V denotes tumor volume and V' denotes convex hull volume</p> | Measures the ratio of the ROI volume contained within the tumor to the calculated convex hull volume |
| | Sphericity | $\text{Sphericity} = \frac{\pi^{\frac{1}{3}} \times (6V)^{\frac{2}{3}}}{A}$ <p>where A denotes area and V denotes tumor volume</p> | Measures the roundness of the ROI |
| | Spherical disproportion | $\text{Spherical disproportion} = \frac{A}{4\pi R^2}$ <p>where R is the radius of a sphere with the same volume as the tumor</p> | Ratio of the surface area of the ROI to the surface area of a sphere with the same volume as the ROI |
| | Maximum 3D diameter | See description in the next column | Measures the maximum 3D ROI diameter. This was measured as the largest pairwise Euclidean distance between surface voxels of the ROI |
| | Surface-to-volume ratio (SVR) | $SVR = \frac{A}{V}$ <p>where A is area and V is volume</p> | Surface-to-volume ratio in ROI |
| | Volume | <p>where R denotes the 3D image resolution</p> $\text{Volume} = R * \text{number of voxels}$ | Volume of the tumor (ROI) |
| | Mass | $\text{Mass} = V * D$ <p>where V denotes the tumor volume, and D denotes the tumor density</p> | Mass of the tumor (ROI) |
| | Density | $\text{Density} = \frac{M}{V}$ <p>where V denotes the tumor volume and M denotes the tumor mass</p> | Density of the tumor (ROI) |
| | Roundness factor (2D) | $\text{Roundness factor} = \frac{4\pi \cdot \text{Area}}{\text{Perimeter}^2}$ | Measure of circularity of a ROI |
| | Eccentricity (2D) | $\text{Eccentricity} = c/a$ <p>where c is the distance from the center to a focus and a is the distance from that focus to a vertex</p> | Measure of how close the tumor shape is to a circle |
| | Solidity (2D) | $\text{Solidity} = \frac{\text{Area}}{\text{Convex area}}$ | Measure of convexity of a ROI on the 2D image |
| GLCM-based features [1] | Auto correlation | $\text{Autocorrelation} = \sum_{i=1}^{N_g} \sum_{j=1}^{N_g} ijP(i, j)$ | Measure of the magnitude of the fineness and coarseness of texture |

| | | |
|--------------------------------------|--|--|
| Cluster tendency | $\text{Cluster tendency} = \sum_{i=1}^{N_g} \sum_{j=1}^{N_g} [i + j - \mu_x - \mu_y]^2 P(i, j)$ | Measure of the homogeneity of the GLCM |
| Maximum probability | $\text{Maximum probability} = \max\{P(i, j)\}$ | Measure of the maximum value of the GLCM matrix |
| Contrast | $\text{Contrast} = \sum_{i=1}^{N_g} \sum_{j=1}^{N_g} i - j ^2 P(i, j)$ | Measures of the local intensity variation of the GLCM |
| Difference entropy | $\begin{aligned} &\text{Difference entropy} \\ &= \sum_{i=0}^{N_g-1} P_{x-y}(i) \log_2 [P_{x-y}(i)] \end{aligned}$ | Measure of the entropy of the processed GLCM matrix P_{x-y} |
| Dissimilarity | $\text{Dissimilarity} = \sum_{i=1}^{N_g} \sum_{j=1}^{N_g} i - j P(i, j)$ | Measure of the difference in each element of the gray level |
| Energy | $\text{Energy} = \sum_{i=1}^{N_g} \sum_{j=1}^{N_g} [P(i, j)]^2$ | Measure of the homogeneity of the GLCM |
| Entropy | $\text{Entropy} = - \sum_{i=1}^{N_g} \sum_{j=1}^{N_g} P(i, j) \log_2 [P(i, j)]$ | Measure of the irregularity of the gray level. |
| Homogeneity | $\text{Homogeneity} = \sum_{i=1}^{N_g} \sum_{j=1}^{N_g} \frac{P(i, j)}{1 + i - j }$ | Measure of the closeness of the gray level. |
| Informational measure of correlation | $\text{IMC} = \text{HXY} - \frac{\text{HXY1}}{\max\{\text{HX}, \text{HY}\}}$ | Secondary measure of homogeneity |
| Variance | $\text{Variance} = \sum_{i=1}^{N_g} \sum_{j=1}^{N_g} (i - \mu_x)^2 P(i, j)$ | Measure of the dispersion of parameter values around the mean of the combinations of reference and neighborhood pixels |

where $P(i, j)$ is the gray level co-occurrence matrix for $(\delta = 1, \alpha = 0)$,

N_g is the number of discrete intensity value in the image,

N is the number of voxels in the ROI,

μ is the mean of $P(i, j)$,

$p_x(i) = \sum_{j=1}^{N_g} P(i, j)$ is the marginal row probabilities,

$p_y(i) = \sum_{i=1}^{N_g} P(i, j)$ is the marginal column probability,

μ_x is the expected value of marginal row probability,

μ_y is the expected value of the marginal column probability,

σ_x is the standard deviation of p_x ,

σ_y is the standard deviation of p_y ,

$p_{x+y}(k) = \sum_{i=1}^{N_g} \sum_{j=1}^{N_g} P(i, j)$, $i + j = k, k = 2, 3, \dots, 2N_g$,

$p_{x-y}(k) = \sum_{i=1}^{N_g} \sum_{j=1}^{N_g} P(i, j)$, $|i - j| = k, k = 0, 1, \dots, N_g - 1$,

$\text{HX} = - \sum_{i=1}^{N_g} P_x(i) \log_2 [p_x(i)]$ is the entropy of P_x ,

$\text{HY} = - \sum_{i=1}^{N_g} P_y(i) \log_2 [p_y(i)]$ is the entropy of P_y ,

$\text{HXY} = - \sum_{i=1}^{N_g} \sum_{j=1}^{N_g} P(i, j) \log_2 [P(i, j)]$ is the entropy of $P(i, j)$

$\text{HXY1} = - \sum_{i=1}^{N_g} \sum_{j=1}^{N_g} P(i, j) \log(p_x(i)p_y(j))$

| | | | |
|------------------------|-----------------------|---|---|
| ISZ-based features [3] | Size-zone variability | $= \frac{1}{\Theta} \sum_{m=1}^M \left[\sum_{n=1}^N P(m, n) \right]^2$ | Variability in the size of the ROI |
| | Intensity variability | $= \frac{1}{\Theta} \sum_{n=1}^N \left[\sum_{m=1}^M P(m, n) \right]^2$ | Variability in the intensity of the ROI |

where $P(m, n)$ is the intensity size zone matrix
 Θ represents the number of homogeneous areas in the tumor,
 M is the number of distinct intensity values,
 N is the size of homogeneous area in the matrix $P(m, n)$

| | | | |
|----------------------------|------------|--|--|
| NGTDM-based features [4,5] | Busyness | $\text{Busyness} = \frac{\sum_{i=1}^L p_i s(i)}{\sum_{i=1}^L \sum_{j=1}^L (ip_i - jp_j)}$ | Measure of the spatial rate of gray-level change |
| | Coarseness | $\text{Coarseness} = \left[\sum_{i=1}^L p_i s(i) \right]^{-1}$ | Measure of edge density |
| | Complexity | $\text{Complexity} = \frac{\sum_{i=1}^L \sum_{j=1}^L \{(i - j) / (n^2 (p_i + p_j)) \} \{ P_i s(i) + P_j s(j) \}}{\sum_{i=1}^L s(i)}$ | Measure of the amount of information in an ROI (gray-level intensities, number of sharp edges) |
| | Contrast | $\text{Contrast} = \frac{1}{N_g(N_g - 1)} \sum_{i=1}^L \sum_{j=1}^L p_i p_j (i - j)^2 \cdot \frac{1}{n^2} \sum_{i=1}^L s(i)$ | Measure of local variations and spread of matrix values |
| | Strength | $\text{Strength} = \frac{\sum_{i=1}^L \sum_{j=1}^L (p_i + p_j) (i - j)^2}{\sum_{i=1}^L s(i)}$ | |

where p_i is the probability of occurrence of a gray level value, $s(i)$ is the NGTDM, N_g is the total number of different gray levels in the ROI, and L is the number of possible gray levels

| | | | |
|---------------------------------|--------------------------|---|---|
| Filter-based features [2] (LoG) | Mean | $\text{Mean} = \frac{1}{N} \sum_i^N G(i)$ <p>where G denotes the filtered 3D image matrix with N voxels.</p> | Measurement of the mean of the ROI image processed by the LoG filter |
| | Max | $\text{Max} = \text{Max}(G(i))$ <p>where G denotes the filtered 3D image matrix with N voxels.</p> | Measurement of the maximum intensity value of the ROI image processed by the LoG filter |
| | Min | $\text{Min} = \text{Min}(G(i))$ <p>where G denotes the filtered 3D image matrix with N voxels.</p> | Measurement of the minimum intensity value of the ROI image processed by the LoG filter |
| | Median | $\text{Median} = \frac{G(i)}{2}$ <p>where G denotes the filtered 3D image matrix</p> | Measurement of the median intensity value of the ROI image processed by the LoG filter |
| | Standard deviation (Std) | $\text{Std} = \left(\frac{1}{N-1} \sum_{i=1}^N (G(i) - \bar{G})^2 \right)^{1/2}$ <p>where G denotes the filtered 3D image matrix with N voxels.</p> | Measurement of the standard deviation of the ROI image processed by the LoG filter |
| | Skewness | $\text{Skewness} = \frac{E(G - \mu)^3}{\sigma^3}$ <p>where μ is the mean of G, σ is the standard deviation of G, and E is the expectation operator.</p> | Measurement of the skewness of the ROI image processed by the LoG filter |

| | | | |
|-------------------------------------|--|---|---|
| | | $\text{Kurtosis} = \frac{E(G - \mu)^4}{\sigma^4}$ | Measurement of kurtosis of the ROI image processed by the LoG filter |
| | Kurtosis | where μ is the mean of G , σ is the standard deviation of G , and E is the expectation operator. | |
| | | $\text{Uniformity} = \sum_{i=1}^{N_l} P(i)^2$ | Measurement of the uniformity of the ROI image processed by the LoG filter |
| | Uniformity | where P denotes the first-order histogram with N_l discrete intensity levels. | |
| | | $\text{Entropy} = - \sum_{i=1}^{N_l} P(i) \log_2 P(i)$ | Measurement of entropy of the ROI image processed by the LoG filter |
| | Entropy | where P denotes the first-order histogram with N_l discrete intensity levels. | |
| | | $G(x, y, z, \sigma) = I(x, y, z) * \frac{1}{\sigma(\sqrt{2\pi})^3} e^{-\frac{x^2+y^2+z^2}{2\sigma^2}}$ | |
| | | $\sigma = 0.5 - 3.5, 0.5$ increments, where $I(x,y,z)$ is the image and $*$ denotes convolution | |
| | Lacunarity (box-counting method) | See description in the next column | Measure of the texture or distribution of gaps within an image |
| Fractal-based features [6,7] | Dimension (box-counting method) | $\text{Fractal dimension} = \lim_{r \rightarrow 0} \frac{\log(N_r)}{\log(1/r)}$ where N_r is the number of voxels and r is the different side lengths | Fractal dimension that quantifies morphological complexity and provides information on self-similarity properties |
| | Fractal signature dissimilarity (blanket method) | See description in the next column | Measure of tumor heterogeneity |
| | Amplitude mean | | Mean of the amplitude values of all samplings lines |
| | Amplitude standard deviation | | Standard deviation of the amplitude values of all sampling lines |
| | Slope mean | | Mean of the slope values of all sampling lines |
| Sigmoid function-based features [2] | Slope standard deviation | See description in the next column | Standard deviation of the slope values of all sampling lines |
| | Offset mean | | Mean of the offset values of all sampling lines |
| | Offset standard deviation | | Standard deviation of the offset values of all sampling lines |
| | | $\text{Sigmoid}(x) = \frac{A}{e^{B \cdot x} + 1} + C$ | |
| | | where A is the amplitude, B is the slope of the curve, and C is the offset of the curve | |

ISZ, intensity variance and size zone variance value; GLCM, gray-level co-occurrence matrix; NGTDM, neighborhood gray tone difference matrix; LoG, Laplacian of Gaussian.

References

1. Aerts, H.J.; Velazquez, E.R.; Leijenaar, R.T.; Parmar, C.; Grossmann, P.; Carvalho, S.; Bussink, J.; Monshouwer, R.; Haibe-Kains, B.; Rietveld, D.; et al. Decoding tumour phenotype by noninvasive imaging using a quantitative radiomics approach. *Nat. Commun.* **2014**, *5*, 4006.
2. Aerts, H.J.; Grossmann, P.; Tan, Y.; Oxnard, G.R.; Rizvi, N.; Schwartz, L.H.; Zhao, B. Defining a Radiomic Response Phenotype: A Pilot Study using targeted therapy in NSCLC. *Sci. Rep.* **2016**, *6*, 33860.

3. Chong, Y.; Kim, J.H.; Lee, H.Y.; Ahn, Y.C.; Lee, K.S.; Ahn, M.J.; Kim, J.; Shim, Y.M.; Han, J.; Choi, Y.L. Quantitative CT variables enabling response prediction in neoadjuvant therapy with EGFR-TKIs: are they different from those in neoadjuvant concurrent chemoradiotherapy? *PLoS ONE* **2014**, *9*, e88598.
4. Niu, L.; Qian, M.; Yang, W.; Meng, L.; Xiao, Y.; Wong, K.K.; Abbott, D.; Liu, X.; Zheng, H. Surface roughness detection of arteries via texture analysis of ultrasound images for early diagnosis of atherosclerosis. *PLoS ONE* **2013**, *8*, e76880.
5. Davnall, F.; Yip, C.S.; Ljungqvist, G.; Selmi, M.; Ng, F.; Sanghera, B.; Ganeshan, B.; Miles, K.A.; Cook, G.J.; Goh, V. Assessment of tumor heterogeneity: an emerging imaging tool for clinical practice? *Insights Imaging* **2012**, *3*, 573–589.
6. Lennon, F.E.; Cianci, G.C.; Cipriani, N.A.; Hensing, T.A.; Zhang, H.J.; Chen, C.T.; Murgu, S.D.; Vokes, E.E.; Vannier, M.W.; Salgia, R. Lung cancer—a fractal viewpoint. *Nat. Rev. Clin. Oncol.* **2015**, *12*, 664–675.
7. Wang, C.; Subashi, E.; Yin, F.F.; Chang, Z. Dynamic fractal signature dissimilarity analysis for therapeutic response assessment using dynamic contrast-enhanced MRI. *Med. Phys.* **2016**, *43*, 1335–1347.

Publisher’s Note: MDPI stays neutral with regard to jurisdictional claims in published maps and institutional affiliations.



© 2020 by the authors. Licensee MDPI, Basel, Switzerland. This article is an open access article distributed under the terms and conditions of the Creative Commons Attribution (CC BY) license (<http://creativecommons.org/licenses/by/4.0/>).